

**ORIGINAL
RESEARCH**

D.F. Kallmes
Y.H. Ding
D. Dai
R. Kadirvel
D.A. Lewis
H.J. Cloft

A Second-Generation, Endoluminal, Flow-Disrupting Device for Treatment of Saccular Aneurysms

BACKGROUND AND PURPOSE: We report a preclinical study of a second-generation endoluminal device (Pipeline Embolization Device [PED-2]) for aneurysmal occlusion and compare the PED-2 with its first-generation predecessor (PED-1).

MATERIALS AND METHODS: Our Institutional Animal Care and Use Committee approved all studies. The PED-2 is a braided endoluminal, flow-diverting device and was implanted across the necks of 18 elastase-induced aneurysms in New Zealand white rabbits and followed for 1 month ($n = 6$), 3 months ($n = 6$), and 6 months ($n = 6$). A second PED-2 was implanted in the abdominal aorta to cover the origins of the lumbar arteries. Angiographic occlusion rates were documented as complete, near-complete, and incomplete. Parent artery percent diameter stenosis was calculated. Results were compared with a previous publication focused on the PED-1, with use of the same model. We compared ordinal outcomes using Fisher Exact or χ^2 tests. We compared continuous data using analysis of variance.

RESULTS: Occlusion rates (complete and incomplete) for the PED-2 were noted in 17 cases (94%) and 1 (6%), respectively, compared with 9 cases of complete (53%) and 8 (47%) of incomplete occlusion with the PED-1 ($P = .0072$). No incidents of branch artery occlusion or distal emboli in vessels downstream of the parent artery were observed with the PED-2. Parent artery neointimal hyperplasia was minimal in most cases and was significantly less than in the PED-1.

CONCLUSIONS: The PED-2 is a biocompatible and hemocompatible device that occludes saccular aneurysms while preserving the parent artery and small-branch vessels in our animal model.

Endovascular treatment of intracranial aneurysms has been revolutionized by the advent of detachable coils.¹ Incremental advances in the treatment of endovascular aneurysms have been achieved through the use of microballoons² and stents,³ which have expanded the realm of coil therapy to include wide-neck and large aneurysms. In addition, multiple second-generation coils, including those with various shapes⁴ and coatings,^{5,6} have been designed in hopes of improving long-term angiographic outcomes after coil embolization. However, even with these important technical advances, recurrence rates in many case series remain frustratingly high.⁷

Endoluminal devices, in contrast to intrasaccular devices such as coils, have been proposed for treatment of saccular aneurysms. Specifically, covered stents have been applied in limited cases for treatment of intracranial aneurysms.⁸ However, widespread application of covered stents for treatment of these aneurysms has been severely limited. First, these covered stents reportedly are quite stiff and difficult to navigate to the intracranial circulation. Second, in-stent restenosis has not been well studied but, on the basis of data from other vascular beds, remains of concern. Third, the risk of covering and occluding small-branch arteries with resultant ischemic stroke must be considered.

We⁹ and others¹⁰⁻¹¹ recently published preclinical studies

detailing a new approach to endoluminal treatment of aneurysms, without the need for adjunctive, intrasaccular coil embolization. The device described in our own recent publication was composed of a tubular, self-expanding metallic mesh or braid, which was advanced through standard microcatheters and deployed across experimental aneurysms in rabbits. From that initial study, we concluded that the high mesh attenuation achieved across the aneurysmal neck was, in most cases, able to promote stasis and thrombosis of the aneurysmal cavity. Furthermore, the same mesh, when placed across small-branch arteries, allowed continued flow within and patency of these branches. Last, intimal hyperplasia within the device was modest.⁹

The above-mentioned study showed feasibility of our approach by use of a first-generation device. Since publication of that previous manuscript, the device has undergone important developments that, on the basis of data presented below, not only allow improved aneurysmal occlusion rates and diminished neointimal hyperplasia formation, but also continue to preserve the patency of small-branch vessels. The purpose of this current study was to present these data and compare them with our own previous study.

Materials and Methods

Pipeline Embolization Device (PED)

We have previously published a preclinical study that focused on a first-generation endoluminal flow-diverting device, which we termed PED-1 (Pipeline Embolization Device; Chestnut Medical Technologies, Menlo Park, Calif) for that study.⁹ The PED-1 was constructed with a 32-strand braiding machine with stainless steel and platinum wire. A second-generation device, termed PED-2 for our present study, constructed with a 48-strand braiding device and composed of

Received October 27, 2008; accepted after revision December 30.

From the Department of Radiology, Mayo Clinic, Rochester, Minn.

This study was funded by Chestnut Medical Technologies. Chestnut Medical Technologies had no editorial authority of drafting, editing, or approving this study.

Please address correspondence to David F Kallmes, MD, Department of Radiology, Mayo Clinic, 200 First St SW, Rochester, MN 55905; e-mail: Kallmes.david@mayo.edu

DOI 10.3174/ajnr.A1530

chromium cobalt and platinum, was evaluated in the current study. The PED-1 afforded approximately 30% area coverage over the aneurysmal neck when fully expanded, whereas the PED-2 achieved 35% coverage.

The PED-2 is attached to a flexible delivery wire, which has radiopaque end markers, and is packaged in an introducer sheath. This packaged device can be loaded into standard microcatheters of 0.027-inch inner diameter or greater. The device is pushed through the microcatheter and is deployed by a combination of microcatheter withdrawal and forward pressure on the delivery wire. The device undergoes approximately 50% shortening during deployment, depending on diameter of the device and the parent artery.¹⁵

In Vivo Experiments

Aneurysms ($n = 18$) were created and treated with the PED-2 in a similar fashion in female New Zealand white rabbits, as previously described.^{9,12} Two days before embolization, subjects were premedicated with aspirin (10 mg/kg PO) and clopidogrel (10 mg/kg PO); this medication regimen was continued for 1 month after embolization. As in the previous publication, additional devices were placed across the lumbar arteries to assess for patency of these small arteries when covered with the device.¹³ Subjects were observed for 1 month ($n = 6$), 3 months ($n = 6$), and 6 months ($n = 6$). At the time of sacrifice, animals were deeply anesthetized. Digital subtraction angiography (DSA) of the aortic arch and the abdominal aorta was performed. The animals were then euthanized with a lethal injection of pentobarbital. Harvested aneurysms and aorta were immediately fixed in 10% neutral buffered formalin. A single aneurysm, from the 6-month group, was processed for scanning electron microscopy (SEM).

Data Analysis

Angiographic evaluation. Aneurysmal dimensions (neck width, aneurysmal height and width) were determined with DSA measurements, which we adjusted by using an external sizing device of known diameter. Angiographic evaluation was performed for angiograms conducted immediately after device implantation as well as at the presacrifice angiograms.

Immediately after implantation, intra-aneurysmal flow disruption was characterized as grade I (minimal), grade II (mild), grade III (moderate), grade IV (marked), and grade V (complete). The follow-up angiography assessed aneurysmal occlusion with use of a 2-point scale, including grade I complete occlusion and grade II incomplete occlusion. Patency of the branch arteries, including lumbar and vertebral arteries covered by the devices, was assessed at follow-up as well.

Conventional histopathologic processing. Gross inspection of the aneurysm specimens was performed to determine subjectively whether the aneurysms had undergone shrinkage with time on the basis of the shape, volume, and texture of the treated aneurysm. Shrunken aneurysms showed firm, cordlike morphologic features, and the dimensions were remarkably decreased compared with the baseline angiograms. The diameters of the lumbar and vertebral arteries covered by the devices were measured under the dissection microscope at the ostia. After routine tissue processing, the fixed samples were embedded in paraffin. Samples were then cut axially at 1000 μm with use of an Isomet low-speed saw (Buehler, Lake Bluff, Ill). The metal stents were carefully removed under a dissecting microscope. The samples were then re-embedded in paraffin, sectioned at 5 to 6 μm , and stained with hematoxylin-eosin (H&E).

Histomorphometry and analysis. Two experienced observers evaluated the histologic sections, as described in the previous publication.^{9,14} Axial sections were taken from the proximal, middle, and distal portions of the aortic stented segment and from the proximal and distal portions of the aneurysm's parent artery. We performed morphometric measurements using digital planimetry with a calibrated microscope system. The external elastic lamina area, internal elastic lamina (IEL) area, and luminal area were measured. Neointimal thickness was measured as the distance from the inner surface of each stent strut to the luminal border. A vessel injury score was calculated according to the Schwartz method.¹⁵ Calculations made from the morphometric measurements were as follows: Neointimal area = IEL area – injured luminal area; Percent stenosis = (injured luminal area \div IEL area) \times 100; Mean injury score = [(sum of injury scores for each strut) \div number of struts]; Mean neointimal thickness = [(sum of neointimal thickness) \div number of struts].¹⁶

Conventional histopathologic analysis. The tissues within the aneurysmal dome were categorized as 1) unorganized thrombus (fresh thrombus or poorly organized thrombus), 2) organized thrombus or organized tissues (connective tissue, which completely replaced the thrombus within the aneurysm dome), and 3) collagenized connective tissue (diffuse and attenuated collagenous matrix, as well as less cellular and vascularized tissue within the connective tissue). The neointima across the aneurysmal neck was defined as 1) thin neointima (tissues on the stent surface at the neck composed of less than 3 layers of cells, with minimal extracellular matrix deposition) and 2) thick neointima (neointima containing more than 3 layers of cells, with or without noticeable collagenous matrix deposition).

Tissue processing for SEM. Tissues were processed, as previously described.^{9,14}

Statistical analysis. Outcomes from the current study (PED-2) were compared with data previously published for the PED-1 device (the original prototype).⁹ We compared aneurysmal dimensions using a 2-way analysis of variance (ANOVA; Treatment \times Duration; JMP; SAS, Cary NC). We compared aneurysmal occlusion scores using the Fisher Exact test (JMP; SAS). All correlations used Bivariate Fit (JMP; SAS). We then compared the degree of luminal stenosis using a 2-way ANOVA (Treatment \times Duration; JMP; SAS). With this analysis, the possible interaction was checked first; if that was not significant, main effects were examined. We compared injury scores using the Kruskal-Wallis test. All significant analyses requiring further examination underwent a Tukey post hoc test (JMP; SAS).

Results

At all time points and in all subjects, devices were readily tracked to the target location and were deployed as desired.

Aneurysmal Morphometry

A 2-way ANOVA showed no interaction between or among groups for the neck size, width, height, or aspect ratio of the aneurysm (height \div neck; Table 1). However, if the main effect "treatment" (the PED prototype version) was examined and all time points were grouped together, it was determined that the aneurysmal widths for PED-1 (3.7 ± 0.8 mm) were significantly less ($P = .0058$) than the aneurysm widths for PED-2 (4.5 ± 0.8 mm), and the mean height of the aneurysms was significantly greater ($P = .0011$) in PED-2-treated aneurysms (10.5 ± 2.2 mm) than in PED-1-treated aneurysms (7.9 ± 2.0 mm). There were no differences in neck size ($2.9 \pm$

Table 1: Aneurysm description by duration in PED studies 1 and 2*

Time (month/s)	PED-1 Neck (mm)	PED-2 Neck (mm)	PED-1 Width (mm)	PED-2 Width (mm)	PED-1 Height (mm)	PED-2 Height (mm)	PED-1 Aspect Ratio	PED-2 Aspect Ratio
1	2.9 ± 1.5	3.4 ± 1.2	3.6 ± 0.8	4.8 ± 0.9	8.0 ± 2.3	9.8 ± 1.9	3.1 ± 1.0	3.0 ± 0.7
3	2.7 ± 1.2	3.4 ± 1.0	3.8 ± 0.7	4.3 ± 0.8	7.7 ± 2.1	10.1 ± 2.4	3.2 ± 1.5	3.1 ± 0.4
6	3.2 ± 0.7	3.2 ± 0.9	3.8 ± 0.9	4.5 ± 0.9	8.0 ± 2.1	11.6 ± 2.3	2.6 ± 0.8	3.7 ± 0.5

Note.—PED indicates Pipeline Embolization Device.

* Data are represented as the mean ± SD. There were no significant differences.

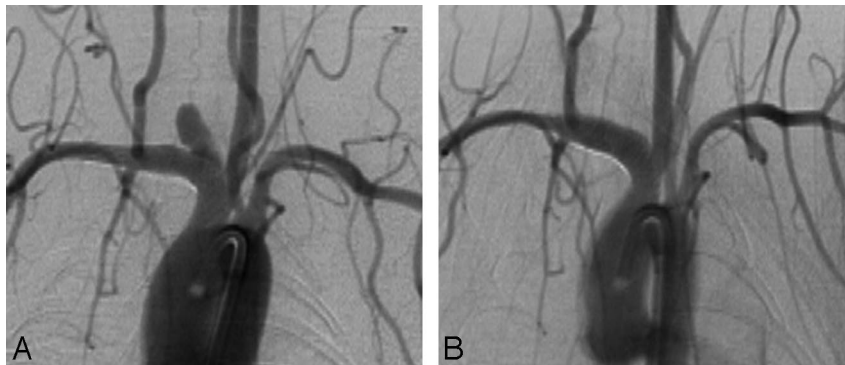


Fig 1. A, DSA immediately after implantation shows that the aneurysm remains completely open to the parent artery. B, This DSA image at 1 month shows that the aneurysm is completely occluded. The distal portion of the parent artery is somewhat narrowed compared with the postimplantation image (A). The right vertebral artery remains patent.



Fig 2. A, This DSA immediately after implantation and (B) 1 month after implantation show near-complete occlusion of the aneurysm cavity at follow-up. The parent artery and the ipsilateral vertebral artery remain patent.

1.1 mm vs 3.3 ± 1.0 mm) or in aspect ratio (2.9 ± 1.1 vs 3.2 ± 0.6) for aneurysms treated with PED-1 vs PED-2, respectively.

Angiographic Outcomes

Aneurysmal occlusion. Intra-aneurysmal flow disruption immediately after implantation was grade I (minimal) in 1 of 18 cases (6%), grade II (mild) in 6 cases (39%), grade III (moderate) in 3 cases (17%), grade IV (marked) in 7 cases (39%), and grade V in 1 case (6%). Aneurysmal neck width ($R^2 = 0.08$; $P = .2572$) did not correlate with immediate postimplantation occlusion score (Bivariate Fit, JMP; SAS), and the aspect ratio (aneurysmal height/neck width) did not correlate ($R^2 = 0.04$, $P = .4045$) with the immediate occlusion score.

At follow-up, 17 (94%) of 18 aneurysms were completely occluded. Angiographically apparent stenosis of the distal portion of the parent artery was noted in a single case, on the order of 20% diameter stenosis (Fig 1). The aneurysm that was not completely occluded (1/18; 6%) had a 1- to 2-mm remnant along its proximal aspect (Fig 2). This remnant occurred in the 1-month group. The occlusion rates were compared with those of the PED-1 device, which demonstrated 9 com-

plete occlusions (53%) and 8 incomplete occlusions (47%). The proportion of aneurysms that were completely occluded was significantly higher with PED-2 compared with PED-1 devices ($P = .0072$; 2-tailed Fisher Exact Test; JMP; SAS).

There were no cases of device migration at follow-up. Two cases also had mild, fusiform dilation of the subclavian artery distal to the aneurysmal neck evident on the pretreatment angiograms. One of these 2 cases showed occlusion of the fusiform lumen external to the PED-2 at follow-up, whereas the other case showed no change in flow within the lumen external to the PED-2 compared with baseline angiography.

Branch artery occlusion. There were no cases of branch artery occlusion, either immediately after implantation or at follow-ups.

Histomorphometry

Aortic devices. Analysis of mean injury scores, a reflection of damage to the vessel by the device, demonstrated a significant interaction (Treatment * Duration; $P = .0140$). A Tukey post hoc analysis showed that the PED-1 group at 3 months (0.2 ± 0.2) generated significantly higher mean injury scores

Table 2: Morphometric measurements in aortic segments

Time (month/s)	PED-1 Injury Score	PED-2 Injury Score	PED-1 Neointimal Thickness (mm)	PED-2 Neointimal Thickness (mm)	PED-1 Area Stenosis (%)	PED-2 Area Stenosis (%)	PED-1 Diameter Stenosis (%)	PED-2 Diameter Stenosis (%)
1	0.0 ± 0.0*	0.0 ± 0.0	0.2 ± 0.1	0.1 ± 0.0	20 ± 5	10 ± 5	10 ± 3	7 ± 2
3	0.3 ± 0.2	0.0 ± 0.0*	0.2 ± 0.1	0.1 ± 0.0	16 ± 5	9 ± 3	13 ± 11	6 ± 1
6	0.1 ± 0.2	0.1 ± 0.0	0.1 ± 0.0	0.1 ± 0.0	15 ± 6	8 ± 2	9 ± 3	5 ± 2

Note:—Data are represented as the mean ± SD. There was a significant ($P = .0128$) mean injury score interaction. * Indicates a significant difference between the * value and the PED-1 at 3 months' value (Tukey post hoc test).

Table 3: Morphometric measurements in aneurysm-bearing arterial segments

		1 Month		3 Months		6 Months	
		Proximal	Distal	Proximal	Distal	Proximal	Distal
Injury score	PED-1	0.0 ± 0.0 ($n = 2$)	0.1 ± 0.2 ($n = 6$)	0.1 ± 0.1 ($n = 3$)	0.1 ± 0.2 ($n = 4$)	0.0 ± 0.0 ($n = 4$)	0.1 ± 0.1 ($n = 6$)
	PED-2	0.0 ± 0.0 ($n = 4$)	0.0 ± 0.0 ($n = 6$)	0.0 ± 0.0 ($n = 6$)	0.0 ± 0.0 ($n = 6$)	0.0 ± 0.0 ($n = 3$)	0.0 ± 0.0 ($n = 5$)
Neointimal thickness (mm)	PED-1	0.2 ± 0.1 ($n = 2$)	0.2 ± 0.0 ($n = 6$)	0.2 ± 0.0 ($n = 3$)	0.1 ± 0.0* ($n = 4$)	0.2 ± 0.1 ($n = 4$)	0.1 ± 0.0* ($n = 6$)
	PED-2	0.2 ± 0.0 ($n = 4$)	0.1 ± 0.0* ($n = 6$)	0.1 ± 0.0 ($n = 6$)	0.1 ± 0.0 ($n = 6$)	0.1 ± 0.0 ($n = 3$)	0.1 ± 0.0 ($n = 5$)
Maximal area stenosis (%)	PED-1	22 ± 2 ($n = 5$)	38 ± 13 ($n = 6$)	35 ± 18 ($n = 2$)	30 ± 10 ($n = 4$)	23 ± 8 ($n = 4$)	17 ± 8 ($n = 6$)
	PED-2	12 ± 1 ($n = 3$)	22 ± 10 ($n = 6$)	15 ± 3 ($n = 6$)	18 ± 7 ($n = 6$)	16 ± 7 ($n = 3$)	19 ± 5 ($n = 5$)
Maximal diameter stenosis (%)	PED-1	11 ± 5 ($n = 2$)	20 ± 10 ($n = 6$)	17 ± 7 ($n = 3$)	12 ± 3 ($n = 4$)	12 ± 6 ($n = 4$)	11 ± 7 ($n = 6$)
	PED-2	9 ± 0.0 ($n = 1$)	14 ± 6 ($n = 6$)	9 ± 2 ($n = 6$)	10 ± 3 ($n = 6$)	5 ± 2 ($n = 5$)	9 ± 4 ($n = 3$)

Note:—Proximal indicates the proximal end of the stented parent artery; distal, the distal end of the stented parent artery. Data are represented as the mean ± SD. * Indicates a significant difference in neointimal thickness between the distal 1-month PED-1 and other distal locations ($P < .05$).

than the PED-2 at 3 months (0.01 ± 0.04) and the PED-1 at 1 month (0.0 ± 0.0 ; $P < .05$). There were no other significant interactions (Table 2). When the main effect treatment groups (PED-1 vs PED-2) were examined, there were significant differences in mean neointimal thickness (0.15 ± 0.06 mm vs 0.09 ± 0.02 mm; $P = .0007$), percent diameter stenosis ($8\% \pm 4\%$ vs $5\% \pm 1\%$; $P = .0032$), neointimal area (1.4 ± 0.5 mm² vs 0.8 ± 0.2 mm²; $P < .0001$), percent area stenosis ($13\% \pm 4\%$ vs $7\% \pm 3\%$; $P < .0001$), and maximal percent area stenosis ($17\% \pm 6\%$ vs $9 \pm 3\%$; $P < .0001$). In all of these comparisons, PED-2 was superior to PED-1.

Aneurysmal devices, distal portion. The variable neointimal thickness showed a significant interaction ($P = .0370$). A Tukey post hoc analysis revealed that the neointimal thickness with PED-1 (0.2 ± 0.4 mm) at 1 month was significantly greater ($P < .05$) than that for PED-2 at 1 month (0.1 ± 0.02 mm). In addition, neointimal thickness with PED-1 at 1 month was significantly greater than the PED-2 group at 3 months (0.1 ± 0.02 mm) and 6 months (0.1 ± 0.04 mm). There were no other significant interactions (Table 3). The main effect treatment groups showed that the PED-2 neointimal area (1.5 ± 0.7 mm²) was significantly greater than the PED-1 neointimal area (1.0 ± 0.3 mm²; $P = .0039$), and the maximal area stenosis for PED-1 ($28 \pm 14\%$) was significantly greater than that of PED-2 ($20 \pm 7\%$; $P = .0319$).

Aneurysmal devices, proximal portion. There were no significant interactions or main effects for this portion of the parent artery (Table 3).

Histologic Outcome

Gross histologic features. At 1 month, 1 of 6 aneurysms had shrunk; at 3 months, 6 of 6 aneurysms had shrunk; and at 6 months, 6 of 6 aneurysms had shrunk.

Histopathologic Features

Aneurysmal neck and dome histologic findings. At 1 month, the dominant findings in the aneurysmal dome were an unorganized thrombus in 5 cases and densely organized

tissue in 1 case. Thick neointima was seen in 4 cases and thin neointima in 2 cases. At 3 months, all aneurysmal domes were filled with attenuated connective tissue. Thick neointima was seen in 4 cases and thin neointima in 2 cases. At 6 months, all 5 aneurysms were filled with collagenized attenuated connective tissue. Thick, collagenized neointima was seen in 3 cases and thin-moderate, collagenized neointima in 2 cases.

Branch vessel histologic findings. All branch vessels that had a PED-2 device across their ostia were patent at all time points. Vertebral artery mean diameters, expressed as the mean ± SD (with the range in parentheses), for the 1-month, 3-month, and 6-month groups were 1.4 ± 0.5 mm (range, 1–2 mm), 1.4 ± 0.5 mm (range, 1–2 mm), and 1.3 ± 0.4 mm (range, 1–2 mm), respectively, whereas the lumbar artery diameters for the 1-month, 3-month, and 6-month groups were 0.8 ± 0.5 mm (range, 0.1–2.0 mm), 0.9 ± 0.4 mm (range, 0.2–1.5 mm), and 0.8 ± 0.3 mm (range, 0.3–1.1 mm), respectively. The neointima across the origins of the branch vessels seemed to be discontinuous (Fig 3).

SEM findings. The aneurysmal neck was completely occluded with the neointima. The lumbar arteries, vertebral artery, and other branches that had a PED-2 cross the ostia all were patent (Fig 4). The tissue covering the stents at the origin of the lumbar and vertebral arteries was continuous with that of the devices at the aorta and parent artery.

Discussion

In this study, we describe the in vivo, preclinical performance of a second-generation endoluminal device (the PED-2), aimed at aneurysmal occlusion, and compare its performance with that of a first-generation device (the PED-1), data that we recently published.⁹ Compared with our previous study with the PED-1, our current study with the PED-2 demonstrated improved aneurysmal occlusion rates and diminished extent of neointimal hyperplasia. These performance improvements may be related to the materials or design of the new device. Furthermore, the patency of small-branch vessels in the rabbit remained excellent when covered with the new device. These

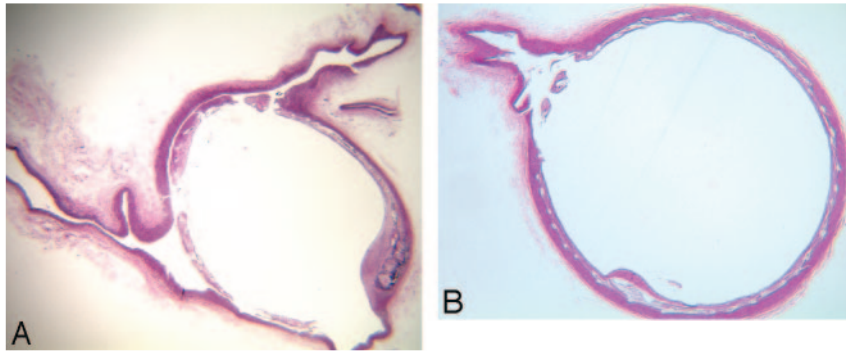


Fig 3. *A*, Photomicrograph (H&E; magnification, $\times 20$) of the vertebral artery. *B*, Photomicrograph (H&E; magnification, $\times 25$) of a lumbar artery. Both the vertebral and lumbar arteries had a device placed across their ostia. The vessels remained patent. The neointima across the origin of each vessel is discontinuous.

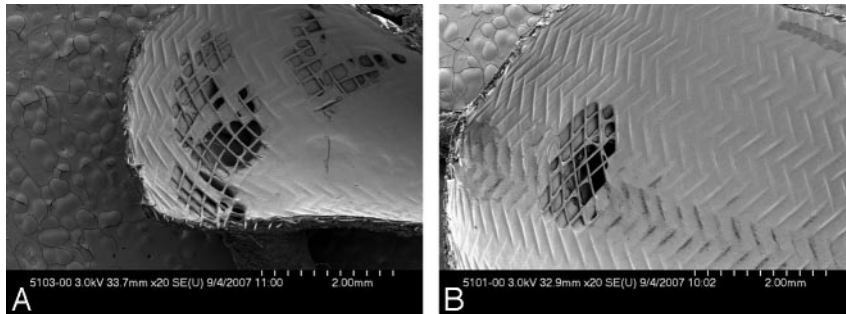


Fig 4. *A*, SEM photograph (magnification, $\times 20$) of the vertebral artery. *B*, An SEM of the ostium of the lumbar artery (magnification, $\times 20$). Both the vertebral and lumbar arteries had a device placed across their ostia. The vessels remained patent. The tissue covering the stents at the origins of branch vessels is continuous with that covering or on the devices at the aorta and parent artery.

new data suggest that the PED-2 offers promise as an effective tool in the treatment of saccular aneurysms.

As in the previous publication,⁹ the patency of small-branch arteries covered by the device was excellent. Most likely, the good patency through the branch vessels is a result of runoff through the vessels. However, these findings in the rabbit do not guarantee that small, perforating arteries in humans will remain patent when covered by the PED-2.

Intimal hyperplasia and in-stent stenosis were minimal in our previous study with the PED-1. The current generation tested in this study produced even less intimal response. We note that the intimal response was greater at the 3-month time point compared with the 6-month time point. This timeframe would correspond to that seen with other stents in other vascular beds, and we would not expect an increase in stenosis at a longer time point.^{17,18}

Unanswered questions remain about the appropriate clinical application of the PED-2. Because the interstrut distance is small, on the order of $0.18 \text{ mm} \times 0.5 \text{ mm}$ for a 4-mm device, the ability to re-enter aneurysms with microcatheters after device deployment will be difficult or impossible. This difficulty will raise questions about how to treat aneurysms that remain patent after treatment with PED-2. Such subsequent treatments will probably be limited to placement of additional PED-2 devices or to open surgery. Some practitioners likely will use the PED-2 in conjunction with intrasaccular coil embolization. In those cases, microcatheters will need to be placed into the aneurysm before deployment of the PED-2. Furthermore, it remains unclear how to interpret the intra-aneurysmal flow after placement of the PED-2 as related to the need for additional treatments. We do not expect that com-

plete aneurysmal occlusion will be achieved immediately after PED-2 placement. We have offered a crude, ordinal scale of immediate postplacement intra-aneurysmal flow disruption in this study and found that, irrespective of these findings, the long-term aneurysmal occlusion rates were excellent.

Our current study had several limitations. We did not include a control group of platinum coils for direct comparison. However, our group has a vast experience with coil occlusion of these model aneurysms, and near-perfect occlusion in a series of this size would be unusual with any coils, including the modified coils that have been introduced for the last 5 years. Second, the aneurysmal neck size and dome dimensions are relatively small compared with those that likely will be treated from a clinical standpoint. We believe that the functional and histologic restoration of the arterial wall at the level of the aneurysmal neck afforded by the PED-2 may portend not only a high rate of complete aneurysmal occlusion, but also a more permanent occlusion.

Conclusions

This preclinical study demonstrates excellent efficacy and safety of a second generation flow diversion device for treatment of saccular aneurysms.

References

1. Molyneux A, Kerr R, Yu L, et al. **International subarachnoid aneurysm trial (ISAT) of neurosurgical clipping versus endovascular coiling in 2143 patients with ruptured intracranial aneurysms: A randomised comparison of effects on survival, dependency, seizures, rebleeding, subgroups, and aneurysm occlusion.** *Lancet* 2005;366:809–17
2. Aletich VA, Debrun GM, Misra M, et al. **The remodeling technique of balloon-**

- assisted Guglielmi detachable coil placement in wide-necked aneurysms: Experience at the University of Illinois at Chicago. *J Neurosurg* 2000;93:388–96
3. Fiorella D, Albuquerque FC, Masaryk TJ, et al. Balloon-in-stent technique for the constructive endovascular treatment of “ultra-wide necked” circumferential aneurysms. *Neurosurgery* 2005;57:1218–27; discussion 1218–27
 4. Vallee JN, Aymard A, Vicaut E, et al. Endovascular treatment of basilar tip aneurysms with Guglielmi detachable coils: Predictors of immediate and long-term results with multivariate analysis 6-year experience. *Radiology* 2003;226:867–79
 5. Cloft HJ. Hydrocoil for endovascular aneurysm occlusion (HEAL) study: periprocedural results. *AJNR Am J Neuroradiol* 2006;27:289–92
 6. Niimi Y, Song J, Madrid M, et al. Endosaccular treatment of intracranial aneurysms using Matrix coils: early experience and midterm follow-up. *Stroke* 2006;37:1028–32
 7. Cloft HJ. Hydrocoil for endovascular aneurysm occlusion (HEAL) study: 3–6 month angiographic follow-up results. *AJNR Am J Neuroradiol* 2007;28:152–54
 8. Saatci I, Cekirge HS, Ozturk MH, et al. Treatment of internal carotid artery aneurysms with a covered stent: Experience in 24 patients with mid-term follow-up results. *AJNR Am J Neuroradiol* 2004;25:1742–49
 9. Kallmes DF, Ding YH, Dai D, et al. A new endoluminal, flow-disrupting device for treatment of saccular aneurysms. *Stroke* 2007;38:2346–52
 10. Ahlhelm F, Roth C, Kaufmann R, et al. Treatment of wide-necked intracranial aneurysms with a novel self-expanding two-zonal endovascular stent device. *Neuroradiology* 2007;49:1023–28
 11. Sadasivan C, Cesar L, Seong J, et al. An original flow diversion device for the treatment of intracranial aneurysms. Evaluation in the rabbit elastase-induced model. *Stroke* 2009;40:952–58
 12. Altes TA, Cloft HJ, Short JG, et al. 1999 ARRS Executive Council Award. Creation of saccular aneurysms in the rabbit: A model suitable for testing endovascular devices American Roentgen Ray Society. *AJR Am J Roentgenol* 2000;174:349–54
 13. Masuo O, Terada T, Walker G, et al. Study of the patency of small arterial branches after stent placement with an experimental in vivo model. *AJNR Am J Neuroradiol* 2002;23:706–10
 14. Dai D, Ding YH, Danielson MA, et al. Modified histologic technique for processing metallic coil-bearing tissue. *AJNR Am J Neuroradiol* 2005;26:1932–36
 15. Schwartz RS, Huber KC, Murphy JG, et al. Restenosis and the proportional neointimal response to coronary artery injury: results in a porcine model. *J Am Coll Cardiol* 1992;19:267–74
 16. Carter AJ, Scott D, Laird JR, et al. Progressive vascular remodeling and reduced neointimal formation after placement of a thermoelastic self-expanding nitinol stent in an experimental model. *Cathet Cardiovasc Diagn* 1998;44:193–201
 17. Asakura M, Ueda Y, Nanto S, et al. Remodeling of in-stent neointima, which became thinner and transparent over 3 years: serial angiographic and angioscopic follow-up. *Circulation* 1998;97:2003–06
 18. Virmani R, Kolodgie FD, Farb A, et al. Drug eluting stents: are human and animal studies comparable? *Heart* 2003;89:133–38